Styrene oxidation catalyzed by $Au_{11}(PPh_3)_7Cl_3$ and $[Au_{11}(PPh_3)_8Cl_2]Cl$ nanoclusters: Impacts of capping ligands, particle size and charge state

Likai Wang[a,b,1], Jin Peng[a,1], Zhenghua Tang[a,c,*], Xiongwu Kang[a], Mingli Fu[c], Shaowei Chen[a,d,**]

[a] *Guangzhou Key Laboratory for Surface Chemistry of Energy Materials, New Energy Research Institute, School of Environment and Energy, South China University of Technology, Guangzhou Higher Education Mega Centre, Guangzhou, 510006, China*
[b] *School of Chemical Engineering, Shandong University of Technology, Zibo, 255049, China*
[c] *Guangdong Provincial Key Laboratory of Atmospheric Environment and Pollution Control, Guangdong Provincial Engineering and Technology Research Center for Environmental Risk Prevention and Emergency Disposal, South China University of Technology, Guangzhou Higher Education Mega Centre, Guangzhou, 510006, China*
[d] *Department of Chemistry and Biochemistry, University of California, 1156 High Street, Santa Cruz, CA, 95064, United States*

A B S T R A C T

Structurally similar molecule-like $Au_{11}(PPh_3)_7Cl_3$ and $[Au_{11}(PPh_3)_8Cl_2]Cl$ nanoclusters have been successfully synthesized and employed as catalysts for selective oxidation of styrene. The two clusters exhibited similar but slightly different well-defined optical absorbance, and the subtle structural difference is also reflected in proton nuclear magnetic resonance (^{1}H NMR) studies. In electrochemical measurements, $Au_{11}(PPh_3)_7Cl_3$ and $[Au_{11}(PPh_3)_8Cl_2]Cl$ show a large electrochemical band gap of 2.15 eV and 2.09 eV, respectively. Styrene oxidation has been employed as a model reaction to investigate the impacts of the ligand shell composition on the catalytic activity and selectivity of the two clusters. Interestingly, the main product is benzaldehyde when oxygen is employed as oxidant, and the catalytic activity of $Au_{11}(PPh_3)_7Cl_3$ is higher than that of $[Au_{11}(PPh_3)_8Cl_2]Cl$. Under the same conditions, the two Au_{11} clusters exhibit much higher catalytic activity than larger clusters (Au_{25}, Au_{38} and Au_{144}) capped with phenylethiolates, as a manifestation of both size influence and surface ligand impacts. In addition, the oxidation efficiency of styrene exhibit a sharp increase when tert-butyl hydroperoxide is utilized as the oxidant, where the catalytic activities of $Au_{11}(PPh_3)_7Cl_3$ and $[Au_{11}(PPh_3)_8Cl_2]Cl$ are comparable with styrene epoxide being the major product. Finally, the twin clusters are either reduced or oxidized to probe the charge effects upon the catalytic reaction, and it was found that the conversion of styrene went up with the charge state from reduced to oxidized for both clusters.

1. Introduction

Whereas bulk gold is catalytically inert [1], nanosized Au particles have been found to exhibit apparent catalytic activity toward various reactions [2–6]. Yet, the mechanistic origin of the catalytic activity has remained largely elusive, mainly due to the structural complexity of the Au nanoparticle catalysts, specifically, the dispersity of the nanoparticle size and various shapes render it difficult to identify the catalytic active sites [7].

Au nanoclusters represent a new type of Au nanoparticles with an ultra-small size (usually less than 2 nm), and more importantly, a molecule-like structure at atomic precision [8–10], such that it is possible to correlate the cluster structures with the catalytic activity provided [11,12]. In fact, in recent years, ligand-protected Au clusters have been found to be catalytically active for various reactions, including CO oxidation [13–15], selective oxidation of styrene [16–21], aerobic oxidation of alcohol [22,23], carbon-carbon coupling reaction[24–26], chemoselective hydrogenation [27,28], as well as electrocatalytic reduction of oxygen [29,30]. For instance, Zhu et. al. studied the catalytic activity of Au_n (n = 25, 38, and 144) clusters in selective oxidation and hydrogenation reactions, and found that the electron-rich kernal was primarily responsible for the catalytic activities [31]. Chen and coworkers employed Au clusters of different sizes (from Au_{11} to Au_{145}) for oxygen reduction reaction, and observed drastic enhancement of the electrocatalytic activity with decreasing core size [29]. However, thus far, little attention has been paid to the effect of the surface ligands, which have been known to affect the core electronic structures and thus may serve as a powerful variable in the manipulation of the catalytic

activity. In a recent study, Li et. al examined the effects of thiolate ligand on the accessibility and catalytic activity of Au clusters, and found that both chain length and functional moiety of the ligand played an important role in catalytic performance, indicating great potential of engineering surface ligand to manipulate the catalytic performance of the Au clusters [32].

Herein, two Au_{11} nanoclusters, $Au_{11}(PPh_3)_7Cl_3$ and $[Au_{11}(PPh_3)_8Cl_2]Cl$, were prepared and their catalytic activity toward styrene oxidation was evaluated and compared within the context of ligand shell composition. The preparation of Au_{11} clusters was first reported in 1966 with triphenylphosphine as the capping ligands [33], but the structure was not clearly determined until 2014 by Hutchison group using X-ray crystallography [34]. The Au_{11} clusters entail a twin of $Au_{11}(PPh_3)_7Cl_3$ and $Au_{11}(PPh_3)_8Cl_3$, which exhibit an almost identical Au core with the latter having one more triphenylphosphine ligand to displace one chloride in the outer space [34]. In the present study, $Au_{11}(PPh_3)_7Cl_3$ and $[Au_{11}(PPh_3)_8Cl_2]Cl$ clusters were synthesized and characterized by UV–vis absorption and proton nuclear magnetic resonance (^{1}H NMR) spectroscopic measurements. Their catalytic performance toward styrene oxidation was examined by using oxygen or TBHP as oxidant, and the impact of the ligand shell composition on the catalytic performance was investigated.

2. Experimental section

2.1. Chemical reagents

Diethyl ether, tetrahydrofuran, *n*-hexane and *n*-pentane were acquired from Caiyunfei Chemical Reagents (Tianjin, China). Hydrogen tetrachloroaurate (III) trihydrate ($HAuCl_4·3H_2O$) and tert-butylhydroperoxide (TBHP) were purchased from Energy Chemicals (Shanghai, China). Sodium borohydride ($NaBH_4$) and triphenylphosphine (PPh_3) were obtained from Aladdin Industrial Corporation (Shanghai, China). The resistivity of the de-ionized water used in this work was 18.3 MΩ cm.

2.2. Synthesis of Au(PPh₃)Cl

White needle crystals of Au(PPh₃)Cl were synthesized from $HAuCl_4·3H_2O$ and PPh_3 by following the procedure reported previously [34]. Typically, 1 g of $HAuCl_4·3H_2O$ was first dissolved in 80 mL of de-aerated ethanol in a 250 mL round-bottom flask. Subsequently, 40 mL of de-aerated ethanol containing 1.33 g of PPh_3 was injected into the above solution under constant stirring at 700 rpm, and white precipitates formed immediately. After stirring for about 30 min, the white precipitates were filtered, washed with diethyl ether for three times, and finally dissolved in CH_2Cl_2. Excess pentane was then added dropwisely into the solution to acquire white needle crystals of Au(PPh₃)Cl.

2.3. Synthesis of Au₁₁ clusters

The synthesis of $Au_{11}(PPh_3)_7Cl_3$ clusters was conducted by following the previously reported approach [34]. Typically, 1 mmol of Au(PPh₃)Cl was first dissolved in 25 mL tetrahydrofuran, and 5.05 mmol of $NaBH_4$ dissolved in absolute ethanol (25 mL) was then added to the above solution under vigorous stirring at 700 rpm. The mixture immediately became dark brown. After stirring for 2 h at ambient temperature, the mixture was precipitated by adding 500 mL of pentane, and the brown precipitate was filtered by a medium-porosity fritted funnel and washed with copious hexanes and CH_2Cl_2/hexanes (1:1) for several times. The precipitates were then dissolved in CH_2Cl_2, and the supernatant was collected by centrifugation and dried by rotary evaporation. This process was repeated for three times to obtain the crude product of $Au_{11}(PPh_3)_7Cl_3$ clusters.

To prepare $[Au_{11}(PPh_3)_8Cl_2]Cl$ clusters, 1 mmol of Au(PPh₃)Cl was

dissolved in 25 mL of CH_2Cl_2, into which was added freshly prepared $NaBH_4$ (0.25 mmol in 3 mL of absolute ethanol) under constant stirring for 24 h. The solvents were then removed by rotary evaporation, and the residual was dissolved in a minimum amount of CH_2Cl_2. Into this solution was then added excess pentane, before the mixture was centrifuged. The supernatant was discarded, and the obtained solids were the crude product of $[Au_{11}(PPh_3)_8Cl_2]Cl$ clusters.

The crude products obtained above were then purified by silica gel column chromatography whereby the nanoclusters were dissolved in CH_2Cl_2, loaded onto the silica gel column, and eluted with a mixture of CH_2Cl_2/CH_3OH (v_{CH2Cl2}/v_{CH3OH} = 25:1–15:1). As a note, the purified Au_{11} clusters can be stable for a few months without change of the characteristic absorbance feature.

2.4. Crystallization of Au₁₁ clusters

In a typical reaction, $Au_{11}(PPh_3)_7Cl_3$ clusters were dissolved in a certain amount of CH_2Cl_2 in a glass vial, into which was then added octane until precipitates were formed in the vial. CH_2Cl_2 was then added into the solution to completely dissolve the precipitates, and the solution was transferred to a bottle containing hexane and sealed with a septum. The bottle was placed in the refrigerator at 4 °C for about one week, leading to the formation of orange needle-shaped crystals of $Au_{11}(PPh_3)_7Cl_3$ clusters. The crystallization of $[Au_{11}(PPh_3)_8Cl_2]Cl$ clusters was conducted in a similar fashion, where red plate-shaped crystals were obtained.

2.5. Preparation of 0.2-Au₁₁(PPh₃)₇Cl₃-SiO₂

Typically, 0.2 mg of $Au_{11}(PPh_3)_7Cl_3$ clusters were dissolved in CH_2Cl_2 solution, while 100 mg of SiO_2 was dispersed in the above solution under stirring, and the mixture was evaporated and vacuum dried at 80 °C for 24 h. Then 100 mg of 0.2-$Au_{11}(PPh_3)_7Cl_3$-SiO_2 was used as catalyst for the selective oxidation of styrene under the same conditions with Au_{11} clusters alone as catalysts. After that, the catalyst was centrifuged, washed with toluene, vacuum dried and recycled.

2.6. Reduction and oxidation of Au₁₁ clusters

Briefly, 2 mg of $Au_{11}(PPh_3)_7Cl_3$ cluster was dissolved in 2 mL of CH_2Cl_2, and then an aqueous solution of $Ce(SO_4)_2$ (2 mL, 1 mg/mL) was added. The mixture was stirred for 1 h, and the obtained nanocluster was denoted as $Au_{11}(PPh_3)_7Cl_3$-ox. With the same procedure but changing $Ce(SO_4)_2$ into $NaBH_4$, $Au_{11}(PPh_3)_7Cl_3$-red was obtained as well. The samples of $[Au_{11}(PPh_3)_8Cl_2]Cl$-ox and $[Au_{11}(PPh_3)_8Cl_2]Cl$-red were also prepared in the similar manner.

2.7. Oxidation of styrene

In a typical reaction, 20 mL of toluene, 1.38 mL of styrene and a certain amount of Au_{11} clusters were added into a 50 mL two-neck round-bottom flask equipped with a reflux condenser. Then the reactor was sealed and purged with oxygen (99.99%), and the solution was stirred at 500 rpm at 100 °C for 24 h. The reaction products were identified by gas chromatography-mass spectrometer (GC–MS), and the conversion of styrene and selectivity of products were determined by ^{1}H NMR analysis. When TBHP was used as oxidant, the catalytic procedures were the same as the above reaction with oxygen. In this work, each experiment was repeated three times.

2.8. Characterizations

UV–vis absorption spectra were acquired with a Shimadzu 2600/2700 spectrophotometer. ^{1}H NMR measurements were conducted by dissolving the Au_{11} clusters in CD_2Cl_2 with a Bruker Ascend 400 MHz spectrometer, with tetramethylsilane (TMS) as internal chemical shift

reference. ^{31}P NMR measurements were performed in the same instrument with CDCl$_3$/CH$_3$OH (2:1) as solvent, and the ^{31}P chemical shift values were referenced to triphenyl phosphate (TPP) by setting the ^{31}P NMR peak of TPP as −17.94 ppm. The Au-to-organic ligand ratios were analyzed by thermogravimetric (TG, METTLER instrument) analysis under a nitrogen flow at the temperature rate of 5 °C/min. The core size of the Au$_{11}$ clusters was analyzed by using a high-resolution transmission electron microscope (HR-TEM, JEOL TEM-2010).

2.9. Electrochemistry

The cyclic and differential pulse voltammograms of the Au$_{11}$ clusters were investigated on Electrochemical workstation (CHI 440E, CH Instruments Inc, Shanghai, China) with a conventional three-electrode cell. A Pt microelectrode (r = 0.25 mm) was employed as the working electrode, while a Pt plate and a Ag/AgCl wire was used as the counter electrode and reference electrode, respectively. Prior to use, the Pt microelectrode was polished with 0.05 μm Al$_2$O$_3$ slurries and sonicated with diluted HNO$_3$ and nanopure water. The Au$_{11}$ clusters were dissolved in CH$_2$Cl$_2$ with 0.1 M tetrabutylammonium perchlorate (TBAP). The concentration of the Au$_{11}$ clusters in CH$_2$Cl$_2$ was 0.1 mM.

3. Results and discussions

The as-prepared Au$_{11}$ clusters was first observed by TEM measurements. Fig. S1 shows the representative TEM image and corresponding size distribution histogram. The average diameter was determined to be ca. 0.75 ± 0.25 nm for Au$_{11}$(PPh$_3$)$_7$Cl$_3$ and ca. 0.77 ± 0.23 nm for [Au$_{11}$(PPh$_3$)$_8$Cl$_2$]Cl. Furthermore, TG measurements (Fig. S2) showed that the organic ligands accounted for 47.3% of the particle weight in Au$_{11}$(PPh$_3$)$_7$Cl$_3$ and 50.5% in [Au$_{11}$(PPh$_3$)$_8$Cl$_2$]Cl, both in good accordance with the respective calculated values (47.2% & 50.4%). The nanoclusters were then characterized by UV–vis spectroscopic measurements. From Fig. 1, two well-defined absorption peaks can be easily identified at 308 nm and 420 nm for Au$_{11}$(PPh$_3$)$_7$Cl$_3$, which shifted slightly to 312 nm and 416 nm for [Au$_{11}$(PPh$_3$)$_8$Cl$_2$]Cl. Such a subtle difference in the absorption profile is due to a change in the core geometry required to accommodate the additional phosphine in [Au$_{11}$(PPh$_3$)$_8$Cl$_2$]Cl [34].

^{1}H NMR measurements were then carried out to probe the organic capping ligands in the Au$_{11}$clusters [35,36]. As depicted in Fig. 2, the Au$_{11}$(PPh$_3$)$_7$Cl$_3$ clusters exhibited three triplets at 7.44, 6.93 and 6.63 ppm, corresponding to the *o*, *p* and *m*-phenyl protons of the PPh$_3$ ligands, respectively. For the [Au$_{11}$(PPh$_3$)$_8$Cl$_2$]Cl clusters, these three protons can be found at slightly different chemical shifts, 7.32, 6.95, and 6.69 ppm, due to different shielding effects from the gold cores.
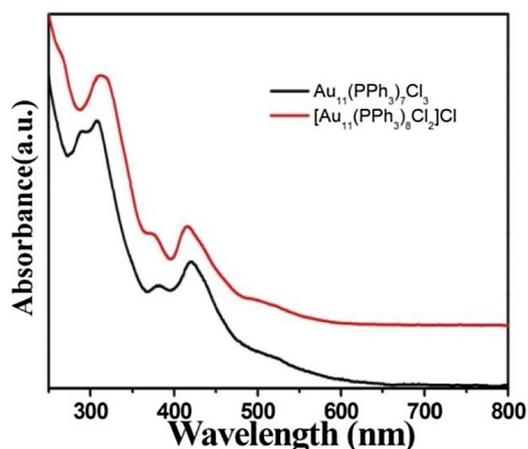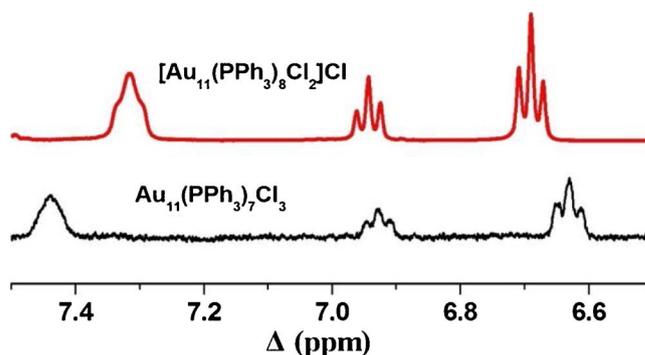

Fig. 2. ^{1}H NMR spectra of Au$_{11}$(PPh$_3$)$_7$Cl$_3$ and [Au$_{11}$(PPh$_3$)$_8$Cl$_2$]Cl clusters in CD$_2$Cl$_2$.

Regardless, for both clusters, the ratio of the integrated areas of these triplets was 2:1:2 for Au$_{11}$(PPh$_3$)$_7$Cl$_3$ and 2:1:2 for [Au$_{11}$(PPh$_3$)$_8$Cl$_2$]Cl, in good agreement with the expected ratio [34].

Furthermore, we also conducted ^{31}P solution NMR of the Au$_{11}$ clusters in comparison of PPh$_3$ and OPPh$_3$ under the same conditions with samples dissolved in CD$_2$Cl$_2$ separately [37]. The ^{31}P spectra can be found in Fig. S3 and all the chemical shift values are summarized in Table S1. One can see that, the chemical shift of ^{31}P is approximately 12.3 and 50.3 ppm for P in PPh$_3$ and OPPh$_3$, respectively, however, once the Au clusters are formed, it shifted to downfield, with a value of 51.0 and 50.8 ppm for P in Au$_{11}$(PPh$_3$)$_7$Cl$_3$ and Au$_{11}$(PPh$_3$)$_8$Cl$_3$, respectively, indicating a dramatic chemical environment change from free molecule to the bound ligand in the clusters. It also ruled out the possibility of forming OPPh$_3$ on the surface of the clusters.

Electrochemical study can offer valuable information related to the physiochemical properties of the molecular Au clusters, especially with regard to electrochemical energy band gap. Subsequently, the electrochemical properties of the Au$_{11}$ clusters were probed. Differential pulse voltammograms (DPV) of the Au$_{11}$ clusters are shown in Fig. S4. Note that, the electrochemical band gap can be derived from the potential gap between the first oxidation peak and the first reduction peak in DPV curves [36,38]. From Fig. S4, the electrochemical band gap of Au$_{11}$(PPh$_3$)$_7$Cl$_3$ and [Au$_{11}$(PPh$_3$)$_8$Cl$_2$]Cl clusters can be estimated as ∼2.15 eV and ∼2.09 eV, respectively. As a note, the band gap of the well-studied Au$_{25}$ cluster was ∼1.3 eV [39], while that of Au$_{38}$ cluster was ∼0.9 eV [38], and no considerable band gap was observed in Au$_{144}$ cluster [40]. Compared with Au$_{25}$, Au$_{38}$, and Au$_{144}$, the twin Au$_{11}$ clusters exhibited substantially higher electrochemical band gap, indicating a markedly stronger quantum confinement effects. The strong quantum confinement effects from the Au$_{11}$ clusters might be beneficial for activating the reacting molecules [41,42].

Interestingly, the Au$_{11}$ clusters exhibited apparent catalytic activity in the selective oxidation of styrene. Note that styrene oxidation is an important reaction, as the products are valuable chemicals used extensively for various applications [31]. With oxygen or TBHP as the oxidant, the reaction is illustrated in Scheme 1, where the oxidation products may entail benzaldehyde, styrene epoxide and acetophenone. Such compositional details, including the conversion of styrene and selectivity of each product, can be revealed by GC–MS and ^{1}H NMR measurements.

Tables 1 and 2 summarize the results of styrene oxidation catalyzed by Au$_{11}$(PPh$_3$)$_7$Cl$_3$ and [Au$_{11}$(PPh$_3$)$_8$Cl$_2$]Cl clusters, respectively. One can see that, for both clusters, with the increase of the catalyst amount from 0.025 to 0.2 mg, the oxidative conversion of styrene increased accordingly; however, a further increase of the cluster amount actually led to a decrease of the conversion ratio. That is, the optimal amount of the catalyst was 0.2 mg, corresponding to a highest conversion of 35.2% and 30.2% styrene for Au$_{11}$(PPh$_3$)$_7$Cl$_3$ and [Au$_{11}$(PPh$_3$)$_8$Cl$_2$]Cl, respectively. In addition, for both clusters catalysts at any loading, the primary product was benzaldehyde, accounting for 63% to 75% among

Fig. 1. UV–vis absorption spectra of Au$_{11}$(PPh$_3$)$_7$Cl$_3$ and [Au$_{11}$(PPh$_3$)$_8$Cl$_2$]Cl clusters in CH$_2$Cl$_2$ solution.

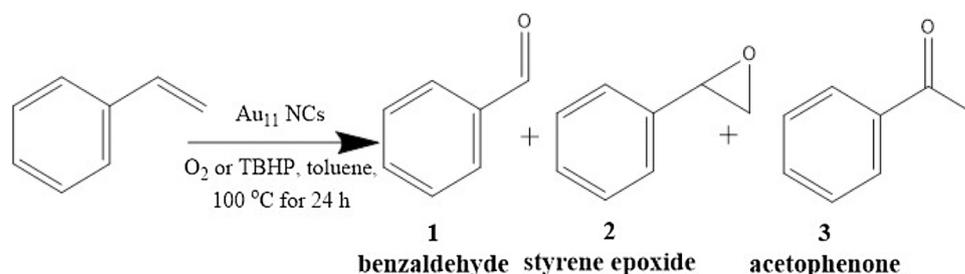**Scheme 1.** Illustration of the selective oxidation of styrene by Au_{11} clusters catalysts.

Table 1
Summary of the selective oxidation of styrene with O_2 catalyzed by different amounts of $Au_{11}(PPh_3)_7Cl_3$.

Catalysts (mg)	Conversion (%)	Selectivity (%)		
		Benzaldehyde	Styrene epoxide	Acetophenone
0.025	22.1 ± 0.3	73.2	21.0	5.8
0.05	31.4 ± 3.4	69.4	27.8	2.8
0.1	33.5 ± 0.6	70.4	24.4	5.2
0.2	35.3 ± 0.6	70.1	27.8	2.1
0.4	30.5 ± 1.4	73.1	19.3	7.6
0.6	24.6 ± 1.3	73.9	23.2	2.9
1.2	24.1 ± 1.0	72.2	24.1	3.7

Table 2
Summary of the selective oxidation of styrene with O_2 catalyzed by different amounts of $[Au_{11}(PPh_3)_8Cl_2]Cl$.

Catalysts (mg)	Conversion (%)	Selectivity (%)		
		Benzaldehyde	Styrene epoxide	Acetophenone
0.025	22.3 ± 0.9	63.2	29.1	7.6
0.05	25.0 ± 0.5	72.0	22.3	5.7
0.1	27.4 ± 1.8	65.8	30.3	3.9
0.2	30.2 ± 1.0	71.1	24.8	4.1
0.4	28.3 ± 2.6	75.2	21.0	3.8
0.6	21.3 ± 1.7	71.4	21.4	7.2
1.2	20.7 ± 2.3	70.9	26.2	2.9

the three products, whereas acetophenone was the minor one at 2% to 8% (Tables 1 and 2). For instance, at the catalyst loading of 0.2 mg, the products included 70.1% benzaldehyde, 27.8% styrene epoxide, and 2.1% acetophenone when $Au_{11}(PPh_3)_7Cl_3$ was used as the catalyst; and for $[Au_{11}(PPh_3)_8Cl_2]Cl$, the products consisted of 71.1% benzaldehyde, 24.8% styrene epoxide, and 4.1% acetophenone. From these results, one can see that the selectivity varied between $Au_{11}(PPh_3)_7Cl_3$ and $[Au_{11}(PPh_3)_8Cl_2]Cl$.

Moreover, at the same catalyst loading, $Au_{11}(PPh_3)_7Cl_3$ displayed a slightly higher conversion than $[Au_{11}(PPh_3)_8Cl_2]Cl$. It indicates that $Au_{11}(PPh_3)_7Cl_3$ possessed slightly better catalytic activity toward styrene oxidation with oxygen as the oxidant. Such a difference of the catalytic performance might originate from the different ligand shell composition. It is well known that the surface gold atoms of the clusters

are the catalytically active sites, and these two molecular clusters have nearly identical Au core. However, $[Au_{11}(PPh_3)_8Cl_2]Cl$ has one more bulky phosphine ligand which probably hinders the access of the substrate to the Au core, resulting in a more effective catalytic activity from the $Au_{11}(PPh_3)_7Cl_3$ clusters.

Interestingly, when TBHP was utilized as the oxidant for styrene oxidation, the catalytic performance was markedly different with O_2 as the oxidant for these two Au clusters [17,43]. The reaction was conducted under the same conditions as those with oxygen as the oxidant. The catalytic results are summarized in Table 3. It can be seen that the styrene conversion efficiency increased significantly to ~70% for both Au_{11} clusters, much higher than those observed in the presence of oxygen (Tables 1 and 2); and styrene epoxide now became the dominant product, accounting for about 80% of the final products, with acetophenone being the second major product (14–16%) and a negligible amount of benzaldehyde (5.6–7.0%), in good consistence with the previous reports [17,43].

Catalytic stability is another important parameter in the evaluation of the catalytic performance. The recyclability of the $Au_{11}(PPh_3)_7Cl_3$ catalyst was evaluated by integrating the $Au_{11}(PPh_3)_7Cl_3$ clusters with SiO_2 support. The composite of 0.2-$Au_{11}(PPh_3)_7Cl_3$-SiO_2 was prepared to conveniently recycle the $Au_{11}(PPh_3)_7Cl_3$ clusters (see experimental section). As depicted in Fig. S5, compared with $Au_{11}(PPh_3)_7Cl_3$ clusters as catalyst, the conversion of styrene decreased from ~35.3% to ~17.3% due to the introduction of SiO_2 as inert support. However, the recycled catalyst of 0.2-$Au_{11}(PPh_3)_7Cl_3$-SiO_2 showed similar activity and selectivity compared with the fresh catalyst (Fig. S5) even after 6 cycles. The results suggest that the 0.2-$Au_{11}(PPh_3)_7Cl_3$-SiO_2 possessed robust catalytic durability, which is of particular importance to put it into real-world use.

In addition to the two Au_{11} clusters, molecular clusters of $Au_{25}(SC_2H_4Ph)_{18}$, $Au_{38}(SC_2H_4Ph)_{24}$ and $Au_{144}(SC_2H_4Ph)_{60}$ were synthesized based on the methods in previous reports [40,44,45]. The UV–vis absorbance profile and the TG results of the three molecular clusters can be found in Figs. S6 and S7. The metal-to-organic ratios agreed well the theoretical values in TG analysis, plus the well-defined characteristic features in absorbance, indicate that molecular clusters of $Au_{25}(SC_2H_4Ph)_{18}$ (denoted as Au_{25} hereafter), $Au_{38}(SC_2H_4Ph)_{24}$ (denoted as Au_{38} hereafter) and $Au_{144}(SC_2H_4Ph)_{60}$ (denoted as Au_{144} hereafter) were successfully obtained. The size effects of the catalyst upon styrene oxidation are compiled in Table 4 with a catalyst loading of 0.2 mg and oxygen as the oxidant. As expected, the conversion decreased with the increase of the core size of the Au clusters, and $Au_{11}(PPh_3)_7Cl_3$ displayed the highest conversion value of 35.3%.

Table 3
Summary of styrene oxidation results with TBHP catalyzed by $Au_{11}(PPh_3)_7Cl_3$ and $[Au_{11}(PPh_3)_8Cl_2]Cl$.

Oxidant	Catalysts	Conversion (%)	Selectivity (%)		
			Benzaldehyde	Styrene epoxide	Acetophenone
TBHP	$Au_{11}(PPh_3)_7Cl_3$	69.7 ± 1.6	7.0	76.3	16.7
TBHP	$[Au_{11}(PPh_3)_8Cl_2]Cl$	69.5 ± 0.3	5.6	80.4	14.0

Table 4
Summary of the catalytic performance of different Au clusters in the selective oxidation of styrene with O_2.

Catalysts	Conversion (%)	Selectivity (%)		
		Benzaldehyde	Styrene epoxide	Acetophenone
$Au_{25}(SCH_2CH_2Ph)_{18}$	26.0 ± 0.2	70.3	27.3	2.4
$Au_{38}(SCH_2CH_2Ph)_{24}$	21.9 ± 1.5	72.7	24.0	3.1
$Au_{144}(SCH_2CH_2Ph)_{60}$	19.5 ± 2.2	74.6	23.0	2.4

Table 5
The catalytic performance of $Au_{11}(PPh_3)_7Cl_{3\text{-red}}$, $[Au_{11}(PPh_3)_8Cl_2]Cl_{\text{-red}}$, $Au_{11}(PPh_3)_7Cl_{3\text{-ox}}$ and $[Au_{11}(PPh_3)_8Cl_2]Cl_{\text{-ox}}$ as catalysts for the selective oxidation of styrene with O_2.

Catalysts	Conversion (%)	Selectivity (%)		
		Benzaldehyde	Styrene epoxide	Acetophenone
$Au_{11}(PPh_3)_7Cl_{3\text{-red}}$	15.5 ± 1.1	72.9	19.6	7.5
$[Au_{11}(PPh_3)_8Cl_2]Cl_{\text{-red}}$	16.0 ± 0.1	76.7	19.6	3.7
$Au_{11}(PPh_3)_7Cl_{3\text{-ox}}$	53.8 ± 0.9	80.0	16.0	4.0
$[Au_{11}(PPh_3)_8Cl_2]Cl_{\text{-ox}}$	13.3 ± 0.6	72.5	21.7	5.8

Interestingly, the selectivity of the three products catalyzed by different clusters is similar or comparable. As a note, the catalytic capability of the $Au_{25}(SC_2H_4Ph)_{18}$, $Au_{38}(SC_2H_4Ph)_{24}$ and $Au_{144}(SC_2H_4Ph)_{60}$ clusters have also been examined by Jin group, where strong core size effects were observed [31]. Our findings agree well with their results, and perfectly highlight the "less-is-more" principle in nanogold catalytic regime [46]. Such size effects have also been observed for ultra-small Au clusters in other catalytic reactions such as CO oxidation [47], alcohol oxidation [48], oxygen reduction reaction [29,30], and so on. The ultrasmall size induced large electrochemical band gap from the twin Au_{11} clusters is probably favorable for activating the reacting substrates [41,42]. Besides the size effect, the nature of the surface ligand might also play an important role in the markedly higher catalytic activity of the two Au_{11} clusters than Au_{25}, Au_{38} and Au_{144} clusters.

Compared with relatively larger Au clusters, the high catalytic activity from the Au_{11} clusters toward styrene oxidation can be attributed to the higher density of Au-atoms with low coordination numbers on the surface of the Au core [29,49]. Note that, several density functional theory investigations have shown that, with the decreasing of core size dimension of Au clusters, the d bands are narrowed and shifted to Fermi level, which are favorable for the adsorption of styrene and oxygen molecules [50–52]. As for the product selectivity difference between oxygen and TBHP as oxidant, it perhaps can be ascribed to different reaction pathways. Previous density functional theory calculations show that, when employing sub-nanometer Au clusters (Au20–Au35) as catalyst and oxygen as oxidant, the formation of a metastable four-membered ring CCOO* intermediate may lead to the high selectivity of benzaldehyde [53], while styrene epoxide dominates the products through an epoxidation process via a surface oxametallacycle intermediate [52,54]. However, the exact reaction pathway by using Au_{11} clusters as catalysts are still unknown, and further efforts on theoretical calculations are urgently needed.

As for the catalytic performance difference from the $Au_{11}(PPh_3)_7Cl_3$ and $[Au_{11}(PPh_3)_8Cl_2]Cl$ clusters with oxygen, it is probably attributed to the one more phosphine ligand induced steric effect that hinder the access of the substrates of the catalytic reaction.

Finally, to further probe the impact of the charge state upon the catalytic performance, the Au_{11} clusters were either reduced or oxidized. The absorbance spectra of the oxidized and reduced Au_{11} clusters can be found in Fig. S8. Interestingly, for the reduced Au_{11} clusters, the main characteristic feature remained for both $Au_{11}(PPh_3)_7Cl_3$ and $[Au_{11}(PPh_3)_8Cl_2]Cl$, suggesting the Au core was probably unchanged. However, upon oxidation, the well-defined absorbance features no longer exist, indicating there is a possibility that the Au_{11} cores probably decomposed or destroyed for both clusters. ^{1}H NMR and ^{31}P NMR analysis of the oxidized and reduced Au_{11} clusters were further conducted. The ^{1}H NMR comparison spectra of the parent, reduced and oxidized Au_{11} clusters are shown in Fig. S9. For the reduced $Au_{11}(PPh_3)_7Cl_3$ and $[Au_{11}(PPh_3)_8Cl_2]Cl$ clusters, the well-defined feature remained, while the chemical shift values from the oxidized Au11 clusters significantly changed. Fig. S3 summarizes the ^{31}P NMR spectra of the parent, reduced and oxidized Au_{11} clusters, along with PPh$_3$ and OPPh$_3$. Apparently, upon either reduction or oxidation, no free PPh$_3$ ligand was generated and no OPPh$_3$ was formed. The chemical shift of

^{31}P remained unchanged, suggesting the PPh$_3$ groups are still attached to the Au surface. Since NMR signal is highly sensitive to its local chemical environment, from NMR analysis, the reduced Au_{11} clusters probably still possessed the Au_{11} core structure, but for the oxidized ones, the possibility of forming other Au core structure or the change of Au_{11} core structure still can't be ruled out.

The reduced and oxidized Au_{11} clusters were then employed as catalyst for selective oxidation of styrene with oxygen as the oxidant and the results are summarized in Table 5. Interestingly, the conversion of $Au_{11}(PPh_3)_7Cl_{3\text{-red}}$ and $[Au_{11}(PPh_3)_8Cl_2]Cl_{\text{-red}}$ clusters was ~15.5% and ~16.0%, much lower than that of $Au_{11}(PPh_3)_7Cl_3$ and $[Au_{11}(PPh_3)_8Cl_2]Cl$, respectively, while for the $Au_{11}(PPh_3)_7Cl_{3\text{-ox}}$ and $[Au_{11}(PPh_3)_8Cl_2]Cl_{\text{-ox}}$ clusters, much higher conversion (~53.8% and ~52.5%) were obtained. One may notice that, even if the product selectivity remained almost unchanged, for either $Au_{11}(PPh_3)_7Cl_3$ or $Au_{11}(PPh_3)_8Cl_3$, with the charge state of the cluster increased, the conversion went up, which corresponded well with the previous studies [49,55]. Note that, the charge state of the Au clusters would significantly affect the catalytic performance [49,55]. It has been postulated that, for the reduced Au clusters, more electrons are de-localized in the Au core, while more negative charge on the Au core would slow down the activation of C=C bond of styrene, leading to lower catalytic activity from the reduced Au_{11} clusters.

4. Conclusions

In this work, a twin of molecular Au clusters of $Au_{11}(PPh_3)_7Cl_3$ and $[Au_{11}(PPh_3)_8Cl_2]Cl$ with nearly identical Au core and slightly different ligand shell composition have been successfully synthesized and employed as catalysts for the selective oxidation of styrene. The similar but slightly different structural features of these two clusters were well examined in absorbance and ^{1}H NMR measurements. When using oxygen as the oxidant, higher catalytic activity was achieved for $Au_{11}(PPh_3)_7Cl_3$ clusters due to the weaker steric effects, however, when using strong oxidant of TBHP, the twin clusters exhibited similar catalytic activities. In addition, the Au_{11} clusters exhibited much higher catalytic performance than that of Au_{25}, Au_{38} and Au_{144} clusters, probably due to the combined effects from the smaller size, the larger electrochemical band gap and the nature of the surface ligand. Lastly, we prepared the oxidized and reduced clusters with their structure examined by absorbance and ^{1}H NMR. With the charge state increased from reduced to oxidized, the reaction conversion toward styrene oxidation went up for both clusters. The findings here not only highlight the "less-is-more" principle, but also suggest that the ligand shell composition of the Au clusters can significantly affect the catalytic performance, which is of great values to the fundamental studies of Au nanocatalysts and its potential practical applications.

Acknowledgements

Appendix A. Supplementary data

Supplementary material related to this article can be found, in the online version, at doi:https://doi.org/10.1016/j.apcata.2018.03.001.

References

[1] G.J. Hutchings, M. Brust, H. Schmidbaur, Chem. Soc. Rev. 37 (2008) 1759–1765.
[2] G.C. Bond, P.A. Sermon, Gold Bull. 6 (1973) 102–105.
[3] G.C. Bond, P.A. Sermon, G. Webb, D.A. Buchanan, P.B. Wells, J. Chem. Soc. Chem. Commun. 13 (1973) 444b–445b.
[4] T. Mitsudome, K. Kaneda, Green Chem. 15 (2013) 2636–2654.
[5] C.-J. Jia, Y. Li, H. Bongard, F. Schuth, J. Am. Chem. Soc. 132 (2010) 1520–1522.
[6] J. Han, Y. Liu, R. Guo, J. Am. Chem. Soc. 131 (2009) 2060–2061.
[7] M.-C. Daniel, D. Astruc, Chem. Rev. 104 (2004) 293–346.
[8] R.W. Murray, Chem. Rev. 108 (2008) 2688–2720.
[9] S. Wang, H. Yu, M. Zhu, Sci. China Chem. 59 (2016) 206–208.
[10] Y. Lu, W. Chen, Chem. Soc. Rev. 41 (2012) 3594–3623.
[11] R. Jin, Nanoscale 7 (2015) 1549–1565.
[12] R. Jin, C. Zeng, M. Zhou, Y. Chen, Chem. Rev. 116 (2016) 10346–10413.
[13] X. Nie, H. Qian, Q. Ge, H. Xu, R. Jin, ACS Nano 6 (2012) 6014–6022.
[14] Z. Wu, D.-e. Jiang, A.K.P. Mann, D.R. Mullins, Z.-A. Qiao, L.F. Allard, C. Zeng, R. Jin, S.H. Overbury, J. Am. Chem. Soc. 136 (2014) 6111–6122.
[15] W. Li, Q. Ge, X. Ma, Y. Chen, M. Zhu, H. Xu, R. Jin, Nanoscale 8 (2016) 2378–2385.
[16] M. Turner, V.B. Golovko, O.P.H. Vaughan, P. Abdulkin, A. Berenguer-Murcia, M.S. Tikhov, B.F.G. Johnson, R.M. Lambert, Nature 454 (2008) 981–984.
[17] Y. Liu, H. Tsunoyama, T. Akita, T. Tsukuda, Chem. Commun. 46 (2010) 550–552.
[18] H. Qian, D.-e. Jiang, G. Li, C. Gayathri, A. Das, R.R. Gil, R. Jin, J. Am. Chem. Soc. 134 (2012) 16159–16162.
[19] P. Huang, G. Chen, Z. Jiang, R. Jin, Y. Zhu, Y. Sun, Nanoscale 5 (2013) 3668–3672.
[20] J. Chai, H. Chong, S. Wang, S. Yang, M. Wu, M. Zhu, RSC Adv. 6 (2016) 111399–111405.
[21] G. Li, R. Jin, Catal. Today 278 (Part 2) (2016) 187–191.
[22] S. Yamazoe, K. Koyasu, T. Tsukuda, Acc. Chem. Res. 47 (2013) 816–824.
[23] T. Yoskamtorn, S. Yamazoe, R. Takahata, J.-i. Nishigaki, A. Thivasasith, J. Limtrakul, T. Tsukuda, ACS Catal. 4 (2014) 3696–3700.
[24] J. Lin, H. Abroshan, C. Liu, M. Zhu, G. Li, M. Haruta, J. Catal. 330 (2015) 354–361.
[25] G. Li, H. Abroshan, C. Liu, S. Zhuo, Z. Li, Y. Xie, H.J. Kim, N.L. Rosi, R. Jin, ACS Nano 10 (2016) 7998–8005.
[26] L. Zhimin, A. Hadi, L. Chao, L. Gao, Curr. Org. Chem. 21 (2017) 476–488.
[27] Y. Zhu, H. Qian, B.A. Drake, R. Jin, Angew. Chem. Int. Ed. 49 (2010) 1295–1298.
[28] G. Li, C. Zeng, R. Jin, J. Am. Chem. Soc. 136 (2014) 3673–3679.
[29] W. Chen, S. Chen, Angew. Chem. Int. Ed. 48 (2009) 4386–4389.
[30] L. Wang, Z. Tang, W. Yan, H. Yang, Q. Wang, S. Chen, ACS Appl. Mater. Interfaces 8 (2016) 20635–20641.
[31] Y. Zhu, H. Qian, M. Zhu, R. Jin, Adv. Mater. 22 (2010) 1915–1920.
[32] J. Li, R.R. Nasaruddin, Y. Feng, J. Yang, N. Yan, J. Xie, Chem. Eur. J. 22 (2016) 14816–14820.
[33] L. Malatesta, L. Naldini, G. Simonetta, F. Cariati, Coord. Chem. Rev. 1 (1966) 255–262.
[34] L.C. McKenzie, T.O. Zaikova, J.E. Hutchison, J. Am. Chem. Soc. 136 (2014) 13426–13435.
[35] Z. Tang, B. Xu, B. Wu, M.W. Germann, G. Wang, J. Am. Chem. Soc. 132 (2010) 3367–3374.
[36] Z. Tang, D.A. Robinson, N. Bokossa, B. Xu, S. Wang, G. Wang, J. Am. Chem. Soc. 133 (2011) 16037–16044.
[37] R. Sharma, G.P. Holland, V.C. Solomon, H. Zimmermann, S. Schiffenhaus, S.A. Amin, D.A. Buttry, J.L. Yarger, J. Phys. Chem. C 113 (2009) 16387–16393.
[38] O. Toikkanen, V. Ruiz, G. Ronnholm, N. Kalkkinen, P. Liljeroth, B.M. Quinn, J. Am. Chem. Soc. 130 (2008) 11049–11055.
[39] J.F. Parker, C.A. Fields-Zinna, R.W. Murray, Acc. Chem. Res. 43 (2010) 1289–1296.
[40] H. Qian, R. Jin, Nano Lett. 9 (2009) 4083–4087.
[41] S. Das, A. Goswami, M. Hesari, J.F. Al-Sharab, E. Mikmeková, F. Maran, T. Asefa, Small 10 (2014) 1473–1478.
[42] B. Liu, P. Wang, A. Lopes, L. Jin, W. Zhong, Y. Pei, S.L. Suib, J. He, ACS Catal. 7 (2017) 3483–3488.
[43] Y. Zhu, H. Qian, R. Jin, Chem. Eur. J. 16 (2010) 11455–11462.
[44] M. Zhu, E. Lanni, N. Garg, M.E. Bier, R. Jin, J. Am. Chem. Soc. 130 (2008) 1138–1139.
[45] H. Qian, Y. Zhu, R. Jin, ACS Nano 3 (2009) 3795–3803.
[46] D. Wayne Goodman, Nature 454 (2008) 948–949.
[47] M. Valden, X. Lai, D.W. Goodman, Science 281 (1998) 1647–1650.
[48] Y. Liu, H. Tsunoyama, T. Akita, T. Tsukuda, Chem. Lett. 39 (2010) 159–161.
[49] G. Li, R. Jin, Acc. Chem. Res. 46 (2013) 1749–1758.
[50] J.A. van Bokhoven, J.T. Miller, J. Phys. Chem. C 111 (2007) 9245–9249.
[51] N.S. Phala, E. Steen, Gold Bull. 40 (2007) 150–153.
[52] W. Gao, X.F. Chen, J.C. Li, Q. Jiang, J. Phys. Chem. C 114 (2010) 1148–1153.
[53] S. Lin, Y. Pei, J. Phys. Chem. C 118 (2014) 20346–20356.
[54] Y. Gao, N. Shao, Y. Pei, X.C. Zeng, Nano Lett. 10 (2010) 1055–1062.
[55] Y. Lu, Y. Jiang, X. Gao, W. Chen, Chem. Commun. 50 (2014) 8464–8467.